Energetic contributions to wall-particle depletion forces

P. González-Mozuelos and J. M. Méndez-Alcaraz
Departamento de Física, CINVESTAV-IPN, Avenida IPN 2508, Col. San Pedro Zacatenco, 07300 México, D.F., Mexico
(Received 24 August 2000; published 9 January 2001)

Recently, depletion forces were accounted for by a contraction of the description based on the integral equations theory of simple liquids [Phys. Rev. E **61**, 4095 (2000)]. The extension of those results to the case of inhomogeneous systems is reported here. Besides, the energetic contributions to the wall-particle depletion forces are studied, as they arise as soon as charge is put on some of the components of a binary mixture of hard spheres on the front of a hard wall. By charging the small particles the amplitude of the depletion attraction between wall and large particles is reduced, and can even become a repulsion. A similar effect is observed if an attractive interaction between wall and small particles is present.

DOI: 10.1103/PhysRevE.63.021201 PACS number(s): 61.20.Gy, 82.70.Dd

I. INTRODUCTION

The term depletion forces originally refers to the attraction between two colloidal particles arising when macromolecules are put into the suspension [1,2]. This results from the expulsion of added macromolecules from the gap between two approaching particles, giving rise to an imbalance between the osmotic pressures within the gap and outside it. The phenomenon has been successfully studied in the usual case that the system can be modeled as a binary mixture of hard spheres [3–9]. Therefore, depletion forces have been accepted as a special case of the entropic forces responsible for the rich phase behavior of hard particles systems. However, recent experimental and theoretical results show that depletion forces can be strongly affected if van der Waals or Coulombic interactions are present in the system [10,11]. They may reduce the amplitude of the depletion attraction at contact, or even invert it to a repulsion. As shown by Méndez-Alcaraz and Klein [12], this behavior can be better understood by considering depletion forces as a special case of the more general effective interactions resulting from a contraction of the description of liquid mixtures. Therefore, if certain components of a mixture are not explicitly considered, their influence on the structure of the remaining particles has to be included in the interaction potential. The latter is obtained by demanding the spatial distribution of the remaining particles to be the same as in the original mixture. Technically, this is done by rewriting the Ornstein-Zernike equation for the original mixture as an effective Ornstein-Zernike equation for the remaining particles, and connecting it with the effective interaction potential using an appropriate closure relation. This idea was first implemented by Medina-Noyola and McQuarrie in order to calculate the interaction between two charged macroions immersed in a bath of small counterions and salt ions [13], as well as in further approaches to the same problem [14].

In Ref. [12] Méndez-Alcaraz and Klein studied the depletion forces in homogeneous mixtures of large hard spheres immersed in a bath of charged or uncharged small hard spheres. The behavior near a hard wall was obtained in the dilute limit by indefinitely increasing the diameter of one of the large components of a ternary mixture of hard spheres. That approach, however, is not suitable to describe depletion forces in more general cases of inhomogeneous systems, for example, when the wall has a relief pattern, or when the confining geometry is more complex. The general problem of the theoretical determination of the structure of inhomogeneous colloidal suspensions has received a considerable amount of attention in the last decade. Two main approaches have been considered for the determination of the local concentration of colloidal particles: one based on the implementation of Ornstein-Zernike (OZ) equations for the concentration profile, also known as integral equations methods [15–23], and the other one based on the density functional theory (DFT) [9,24–27]. With regard to the relative merits of each approach it can be said that the DFT methods provide a quantitatively better description of the spatial distribution of particles, but the approach based on the OZ equations is far easier to implement, and also provides a very good qualitative description of the concentration profiles. In particular, the positions of the maxima and minima of those profiles are very well accounted for by the integral equation methods. Even more, the OZ equations are the natural starting point for the implementation of the contraction formalism from which the effective external potentials are determined, as we explain in Sec. II. In that section, we also present a brief discussion about the connection between the DFT and the OZ equations. Our results are then used in Secs. III and IV in order to study the energetic contributions to the wall-particle depletion forces arising from the charging of some of the components of a binary mixture of hard spheres in front of a hard wall. Finally, the paper is closed with a section of conclusions.

II. EFFECTIVE POTENTIALS

The structure of a homogeneous liquid mixture of p spherical components can be determined from the OZ equation [28],

$$\tilde{h}_{ij}(q)=\tilde{c}_{ij}(q)+\sum_{k=1}^{p} n_k \tilde{h}_{ik}(q)\tilde{c}_{kj}(q); \quad i,j=1,\cdots,p, \tag{1}$$

written here in the Fourier space (this feature being indicated by the tilde, as well as by the dependence on the wave num-

 ©2001 The American Physical Society

ber q), complemented with suitable closure relations between $h_{ij}(r)$ and $c_{ij}(r)$ which also involve the corresponding pair potentials $u_{ij}(r)$ and have the general form [28]

$$c_{ij}(r) = -\beta u_{ij}(r) + h_{ij}(r) - \ln[1 + h_{ij}(r)] + b_{ij}(r), \quad (2)$$

with some appropriate approximation for the bridge function $b_{ij}(r)$. The functions $\tilde{h}_{ij}(q)$ and $\tilde{c}_{ij}(q)$ are the total and direct correlation functions, respectively. The coefficients n_k are the partial number densities. With a matrix notation Eq. (1) takes the form

$$\mathbf{H}(q) = \mathbf{C}(q) + \mathbf{C}(q)\mathbf{N}\mathbf{H}(q), \quad (3)$$

where $\mathbf{H}(q)$, $\mathbf{C}(q)$ and $\mathbf{N}$ are symmetric square matrices of components $[\mathbf{H}(q)]_{ij} = \tilde{h}_{ij}(q)$, $[\mathbf{C}(q)]_{ij} = \tilde{c}_{ij}(q)$, and $[\mathbf{N}]_{ij} = n_i \delta_{ij}$.

The structure of liquid mixtures is usually studied by means of experimental techniques that are unable to detect all the components. For example, light scattering experiments do not detect the salt ions nor the water molecules in an aqueous suspension of polystyrene spheres, except for their effects on the structure of the colloidal particles. Therefore, models including the experimentally unobserved species are necessary in order to interpret the experimental results for the observed components. According to this distinction between observed and unobserved components, the matrices appearing in Eq. (3) can be partitioned in blocks,

$$\mathbf{X} = \begin{pmatrix} \mathbf{X}_{AA} & \mathbf{X}_{AB} \\ \mathbf{X}_{BA} & \mathbf{X}_{BB} \end{pmatrix},$$

and Eq. (3) itself can be rewritten as

$$\mathbf{H}_{AA}(q) = \mathbf{C}_{AA}(q) + \mathbf{C}_{AA}(q)\mathbf{N}_{AA}\mathbf{H}_{AA}(q) + \mathbf{C}_{AB}(q)\mathbf{N}_{BB}\mathbf{H}_{BB}(q), \quad (4)$$

$$\mathbf{H}_{BB}(q) = \mathbf{C}_{BB}(q) + \mathbf{C}_{BB}(q)\mathbf{N}_{BB}\mathbf{H}_{BB}(q) + \mathbf{C}_{BA}(q)\mathbf{N}_{AA}\mathbf{H}_{AA}(q). \quad (5)$$

The indices A and B refer to the observed and unobserved subsets, respectively. Solving Eq. (5) for $\mathbf{H}_{BB}(q)$ and substituting the result into Eq. (4) yields

$$\mathbf{H}_{AA}(q) = \mathbf{C}^{\text{eff}}_{AA}(q) + \mathbf{C}^{\text{eff}}_{AA}(q)\mathbf{N}_{AA}\mathbf{H}_{AA}(q), \quad (6)$$

where

$$\mathbf{C}^{\text{eff}}_{AA}(q) = \mathbf{C}_{AA}(q) + \mathbf{C}_{AB}(q)[\mathbf{N}^{-1}_{BB} - \mathbf{C}_{BB}(q)]^{-1}\mathbf{C}_{BA}(q). \quad (7)$$

Equation (6) has the same structure as Eq. (3) and can therefore be interpreted as an effective OZ equation for the observed components. Besides, $\mathbf{C}^{\text{eff}}_{AA}(q)$ can be used together with a closure relation of the general form

$$c^{\text{eff}}_{ij}(r) = -\beta u^{\text{eff}}_{ij}(r) + h_{ij}(r) - \ln[1 + h_{ij}(r)] + b^{\text{eff}}_{ij}(r) \quad (8)$$

in order to obtain the effective interaction potentials $u^{\text{eff}}_{ij}(r)$ between observed particles. This contraction of the description is the origin of depletion forces when the added macromolecules are the unobserved species [12].

In order to extend the previous results to inhomogeneous systems, let us consider a multicomponent fluid of spherical particles subject to the action of external fields. Let $\psi_{wi}(\mathbf{r})$ be the external potential acting on all the particles of species i at position $\mathbf{r}$. The equilibrium local number density of particles of this species at $\mathbf{r}$, denoted by $n_i(\mathbf{r})$, is related to the corresponding external potential by the equation

$$n_i(\mathbf{r}) = z_i \exp(-\beta\psi_{wi}(\mathbf{r}) + c^{(1)}_i[\{n(\mathbf{r})\}, \mathbf{r}]), \quad (9)$$

where z_i is the fugacity of species i, and $c^{(1)}_i[\{n(\mathbf{r})\}, \mathbf{r}]$ is a functional of the local concentration which represents the contribution to the chemical potential due to the interaction of a particle of species i located at $\mathbf{r}$ with all the other particles in the system. The functional $c^{(1)}_i[\{n(\mathbf{r})\}, \mathbf{r}]$ is also the generator of a hierarchy of direct correlation functions defined by

$$c^{(m+1)}_{ij\ldots l}[\{n(\mathbf{r})\}, \mathbf{r}_1, \mathbf{r}_2, \ldots, \mathbf{r}_{m+1}] = \frac{\delta^m c^{(1)}_i[\{n(\mathbf{r})\}, \mathbf{r}_1]}{\delta n_j(\mathbf{r}_2)\cdots\delta n_l(\mathbf{r}_{m+1})}. \quad (10)$$

In particular, $c^{(2)}_{ij}[\{n(\mathbf{r})\}, \mathbf{r}_1, \mathbf{r}_2]$ corresponds to the OZ direct correlation function between species i and j of the nonuniform fluid. Let us also assume that the system is in thermodynamic equilibrium with an infinity reservoir within which $\psi_{wi}(\mathbf{r}) = 0$, for all i. The local concentration of each component is then uniform within the reservoir, n_i being the corresponding bulk number density of species i. Taking the functional Taylor expansion of $c^{(1)}_i[\{n(\mathbf{r})\}, \mathbf{r}_1]$ with respect to the conditions in the reservoir it is found that this can be rewritten as

$$c^{(1)}_i[\{n(\mathbf{r})\}, \mathbf{r}_1] = \ln\frac{n_i}{z_i} + \sum_{j=1}^{p} \int d^3\mathbf{r}_2 c_{ij}(|\mathbf{r}_1 - \mathbf{r}_2|) \times [n_j(\mathbf{r}_2) - n_j] + b_{wi}(\mathbf{r}_1), \quad (11)$$

where $c_{ij}(|\mathbf{r}_1 - \mathbf{r}_2|) = c^{(2)}_{ij}[\{n(\mathbf{r})\} = \{n\}, \mathbf{r}_1, \mathbf{r}_2]$ is the direct correlation function in the reservoir, and the bridge function $b_{wi}(\mathbf{r}_1)$ is the sum of the corresponding third and higher order terms of this expansion. Therefore, Eq. (9) can be rewritten with the form of the OZ equation:

$$h_{wi}(\mathbf{r}) = c_{wi}(\mathbf{r}) + \sum_{j=1}^{p} n_j \int d^3\mathbf{r}' c_{ij}(|\mathbf{r} - \mathbf{r}'|) h_{wj}(\mathbf{r}'); \quad i = 1, \cdots, p, \quad (12)$$

where use has been made of the definitions

$$h_{wi}(\mathbf{r}) \equiv \frac{n_i(\mathbf{r})}{n_i} - 1 \quad (13)$$

and

$$c_{wi}(\mathbf{r}) \equiv -\beta\psi_{wi}(\mathbf{r}) + h_{wi}(\mathbf{r}) - \ln[1+h_{wi}(\mathbf{r})] + b_{wi}(\mathbf{r}). \tag{14}$$

Equations (12) and (14) are the OZ equation for the concentration profile and the general form of its closure relations, respectively. They are exact and provide a general method to calculate the local concentrations of particles induced by external fields, if the direct correlation functions in the reservoir and the functional dependence of $b_{wi}(\mathbf{r})$ are known. In practice, however, it is necessary to introduce some approximations at this level, since this information is usually lacking.

As in the homogeneous case, we can also use a matrix notation here. In Fourier space Eq. (12) leads to

$$\mathbf{H}_w(\mathbf{q}) = \mathbf{C}_w(\mathbf{q}) + \mathbf{C}(q)\mathbf{N}\mathbf{H}_w(\mathbf{q}), \tag{15}$$

where $\mathbf{H}_w(\mathbf{q})$ and $\mathbf{C}_w(\mathbf{q})$ are column vectors with components $[\mathbf{H}_w(\mathbf{q})]_i = \tilde{h}_{wi}(\mathbf{q})$ and $[\mathbf{C}_w(\mathbf{q})]_i = \tilde{c}_{wi}(\mathbf{q})$. The square matrices $\mathbf{C}(q)$ and $\mathbf{N}$ refer to the homogeneous reservoir and are the same as in Eq. (3). This equation can also be partitioned in blocks according to the distinction between observed (A) and unobserved (B) species:

$$\mathbf{H}_{wA}(\mathbf{q}) = \mathbf{C}_{wA}(\mathbf{q}) + \mathbf{C}_{AA}(q)\mathbf{N}_{AA}\mathbf{H}_{wA}(\mathbf{q}) + \mathbf{C}_{AB}(q)\mathbf{N}_{BB}\mathbf{H}_{wB}(\mathbf{q}), \tag{16}$$

$$\mathbf{H}_{wB}(\mathbf{q}) = \mathbf{C}_{wB}(\mathbf{q}) + \mathbf{C}_{BB}(q)\mathbf{N}_{BB}\mathbf{H}_{wB}(\mathbf{q}) + \mathbf{C}_{BA}(q)\mathbf{N}_{AA}\mathbf{H}_{wA}(\mathbf{q}). \tag{17}$$

Solving Eq. (17) for $\mathbf{H}_{wB}(\mathbf{q})$ and substituting the result into Eq. (16) yields

$$\mathbf{H}_{wA}(\mathbf{q}) = \mathbf{C}^{\mathrm{eff}}_{wA}(\mathbf{q}) + \mathbf{C}^{\mathrm{eff}}_{AA}(q)\mathbf{N}_{AA}\mathbf{H}_{wA}(\mathbf{q}), \tag{18}$$

where

$$\mathbf{C}^{\mathrm{eff}}_{wA}(\mathbf{q}) = \mathbf{C}_{wA}(\mathbf{q}) + \mathbf{C}_{AB}(q)[\mathbf{N}^{-1}_{BB} - \mathbf{C}_{BB}(q)]^{-1}\mathbf{C}_{wB}(\mathbf{q}), \tag{19}$$

and $\mathbf{C}^{\mathrm{eff}}_{AA}(q)$ is given by Eq. (7). By analogy with Eq. (14) it seems natural to define the corresponding effective external potentials $\psi^{\mathrm{eff}}_{wi}(\mathbf{r})$ by the equation

$$c^{\mathrm{eff}}_{wi}(\mathbf{r}) \equiv -\beta\psi^{\mathrm{eff}}_{wi}(\mathbf{r}) + h_{wi}(\mathbf{r}) - \ln[1+h_{wi}(\mathbf{r})] + b^{\mathrm{eff}}_{wi}(\mathbf{r}). \tag{20}$$

A suitable approximation for $b^{\mathrm{eff}}_{wi}(\mathbf{r})$ should be used here in order to get a closed set of equations.

In order to calculate the effective external potentials $\psi^{\mathrm{eff}}_{wi}(\mathbf{r})$, we have first to determine the direct correlation functions $c_{ij}(r)$ in the reservoir by solving Eqs. (1) and (2). Then, $c^{\mathrm{eff}}_{wi}(\mathbf{r})$ can be determined according to Eq. (19) by solving Eqs. (12) and (14). Finally, $\psi^{\mathrm{eff}}_{wi}(\mathbf{r})$ can be determined by means of Eq. (20). In the process, some approximations for the bridge functions $b_{ij}(r), b_{wi}(\mathbf{r})$ and $b^{\mathrm{eff}}_{wi}(\mathbf{r})$ must be introduced. The kind of approximations used in this work will be discussed in Sec. III.

III. MODEL AND APPROXIMATIONS

In order to model suspended hard spheres (labeled here as species 1) and charged or uncharged macromolecules (species 2) on the front of a hard wall we take the interparticle interaction potential

$$\beta u_{ij}(r) = +\infty \quad \text{for } r < \sigma_{ij} \equiv \frac{\sigma_i + \sigma_j}{2},$$

$$= K_{ij}\frac{\mathrm{e}^{-\kappa r}}{r} \quad \text{for } r \geqslant \sigma_{ij}, \tag{21}$$

and the potential

$$\beta\psi_{wi}(x) = +\infty \quad \text{for } x < \frac{\sigma_i}{2},$$

$$= K_{wi}\mathrm{e}^{-\kappa x} \quad \text{for } x \geqslant \frac{\sigma_i}{2} \tag{22}$$

between particles and wall, σ_i being the diameter of the component i. The values $K_{11} = K_{12} = K_{21} = K_{w1} = 0$ ensure the hard core interaction between the colloidal particles, and between them and the other components (polymer coils and wall). By taking $K_{22} \geqslant 0$ the macromolecules are modeled as Yukawa spheres, which assumes that the polymer concentration is within the highly dilute regime and that the ionic concentration is high enough to consider that the configuration of each coil is basically globular. It should be noted that the Yukawa model is itself an effective potential resulting from the contraction of the solvent molecules and of the small ions (counterions and salt ions) from the description of the original system; their effects are contained in K_{22} and in κ. In addition, K_{22} goes as the square of the charge of the coils [13,14]. Furthermore, by taking $K_{w2} \neq 0$, a Coulombic interaction between coils and wall is accounted for within the Yukawa model; the value of K_{w2} depends on the product of the charge of the polymer coils and the surface charge density on the wall [15]. Moreover, Eq. (22) can also be seen as a rough model for polymer-wall van der Waals interactions, with K_{w2} staying for the Hamaker constant, and κ accounting for the range of the potential.

The wall-particle depletion potential $\psi^{\mathrm{eff}}_{w1}(x)$ is obtained by taking the polymer coils out of the picture. It is done here within the mean spherical approximation (MSA) [28]:

$$h_{w1}(x) = -1 \quad \text{for } x < \frac{\sigma_1}{2},$$

$$c^{\mathrm{eff}}_{w1}(x) = -\beta\psi^{\mathrm{eff}}_{w1}(x) \quad \text{for } x \geqslant \frac{\sigma_1}{2}, \tag{23}$$

obtained from Eq. (20) after neglecting $b^{\mathrm{eff}}_{w1}(x)$ and linearizing the logarithm. With Eq. (19), it leads to $\beta\psi^{\mathrm{eff}}_{w1}(x) = +\infty$ for $x < \sigma_1/2$ and

$$\beta\psi_{w1}^{\mathrm{eff}}(x) = -c_{w1}(x) - 2\pi n_2 \int_{-\infty}^{\infty} dx' c_{w2}(x') \times \int_{|x-x'|}^{\infty} ds\, s\, \mathcal{F}^{-1}\left\{ \frac{\tilde{c}_{21}(q)}{[1-n_2\tilde{c}_{22}(q)]} \right\} \quad (24)$$

for $x \geqslant \sigma_1/2$, where the involved integral was rewritten in a simple form [29] ($\mathcal{F}^{-1}$ denotes an inverse Fourier transform). When the system consists only of hard objects ($K_{22} = K_{w2} = 0$) we get for the infinite dilute limit of n_1, up to linear terms in n_2,

$$\beta\psi_{w1}^{\mathrm{eff}}(x) = -2\pi n_2 \int_{-\infty}^{\infty} dx' c_{w2}(x') \int_{|x-x'|}^{\infty} ds\, s\, c_{21}(s), \quad (25)$$

with $c_{21}(r) = -1$ for $r < \sigma_{21}$ and 0 elsewhere, and $c_{w2}(x) = -1$ for $x < \sigma_2/2$ and 0 elsewhere. After integratting this equation we recover the Asakura-Oosawa potential for a particle near a hard wall [12], a result also derived by Götzelmann *et al.* [7] by a rather different method:

$$\beta\psi_{w1}^{\mathrm{eff}}(h) = -\varphi_2 \left(\frac{h}{\sigma_2} - 1 \right)^2 \left(1 + 3\frac{\sigma_1}{\sigma_2} + 2\frac{h}{\sigma_2} \right) \quad (26)$$

for $0 \leqslant h < \sigma_2$ and 0 for larger distances. Here, $h = x - \sigma_1/2$ is the distance from the surface of one particle of species 1 to the wall, and $\varphi_i = \pi n_i \sigma_i^3/6$ the volume fraction of species i. Expression (26) has been found to be an excellent approximation by comparison with direct measurements of depletion potentials in inhomogeneous mixtures of colloid and nonionic polymers [30]. In the same dilute limit it is also possible to get analytical results for $\beta\psi_{w1}^{\mathrm{eff}}(x)$ when $K_{w2} \neq 0$ by putting in Eq. (25) $c_{w2}(x) = -1$ for $x < \sigma_2/2$ and $-K_{w2}\mathrm{e}^{-\kappa x}$ for $x \geqslant \sigma_2/2$. However, such approximations become inappropriate since they neglect the correlation between coils, which may be dominant when charge is present.

In the general case we use Eq. (18) for $x \geqslant \sigma_1/2$, rewritten in the form [29]

$$\beta\psi_{w1}^{\mathrm{eff}}(x) = -h_{w1}(x) - 2\pi n_1 \int_{-\infty}^{\infty} dx' h_{w1}(x') \times \int_{|x-x'|}^{\infty} ds\, s\, c_{11}^{\mathrm{eff}}(s) \quad (27)$$

instead of Eq. (24), since in this way we avoid calculating $c_{wi}(x)$ for $x < \sigma_i/2$. An accurate input for the correlation functions in Eq. (27) is necessary. We determine them by using MSA for the correlations involving hard spheres:

$$h_{11,12}(r) = -1 \quad \text{for } r < \sigma_{11,12},$$

$$c_{11,12}(r) = -\beta u_{11,12}(r) \quad \text{for } r \geqslant \sigma_{11,12}, \quad (28)$$

and the hypernetted chain approximation (HNC) [28] for the charged component:

$$c_{22}(r) = -\beta u_{22}(r) + h_{22}(r) - \ln[1 + h_{22}(r)]. \quad (29)$$

Combined with Eq. (1), these closures provide a complete set of integral equations that we numerically solve for $c_{11}(r)$, $c_{12}(r) = c_{21}(r)$, and $c_{22}(r)$ by means of a five parameters version of the Ng method [31]. The wall-particle correlations are then obtained from Eq. (12) by using also MSA:

$$h_{w1,2}(x) = -1 \quad \text{for } x < \frac{\sigma_{1,2}}{2},$$

$$c_{w1,2}(x) = -\beta\psi_{w1,2}(x) \quad \text{for } x \geqslant \frac{\sigma_{1,2}}{2}. \quad (30)$$

The resulting equations are linear and we solve them for $c_{w1}(x)$ and $c_{w2}(x)$ by means of the same numerical scheme applied in previous works [15]. In Sec. IV we present the results obtained from the scheme resumed here, varying the different parameters that characterize this model in order to analyze their impact on the general behavior of $\beta\psi_{w1}^{\mathrm{eff}}(x)$.

IV. RESULTS AND DISCUSSION

All the effective wall-particle potentials presented in this section correspond to a size ratio $\sigma_1/\sigma_2 = 10$ and to a dimensionless screening parameter $\kappa\sigma_2 = 1.38$, which are typical values. The results shown in Figs. 1(a) and 1(b) correspond to the infinite dilute limit of macroparticles ($\varphi_1 = 0$) in front of a neutral wall ($K_{w2} = 0$) for two different concentrations of unobserved particles: $\varphi_2 = 0.008$ and $\varphi_2 = 0.02$, respectively. They illustrate the process in which the electrostatic repulsion between the polymer globules is increased, starting with neutral coils ($K_{22} = 0$, solid line), passing through $K_{22} = 10$ (dashed line) and $K_{22} = 50$ (dotted line), and finally reaching $K_{22} = 156$ (circles). It can be immediately appreciated that during the charging process the effective wall-macroparticle potential $\beta\psi_{w1}^{\mathrm{eff}}(x)$ becomes more structured, i.e., longer ranged and with wider oscillations. In particular, the attractive well at contact ($x = \sigma_1/2$) that this potential exhibits when $K_{22} = 0$ is gradually transformed into a repulsive barrier when the repulsion among the unobserved particles is incremented. This last feature is attributable to the increased concentration of small particles in the immediate vicinity of the wall induced by the electrostatic pushing exerted by the remaining small particles, i.e., those located farther from the wall, a characteristic that has been described in previous works [15].

From the comparison of Figs. 1(a) and 1(b) it also becomes clear that the effects described above are even more noticeable for higher concentrations of polymer globules. This complementary process is more clearly illustrated in Fig. 2, which again presents the results corresponding to an infinite dilution of macroparticles ($\varphi_1 = 0$) in front of a neutral wall ($K_{w2} = 0$), but explicitly showing the evolution of $\beta\psi_{w1}^{\mathrm{eff}}(x)$ when the pair interaction among the unobserved particles is kept fixed [$K_{22} = 0$ in Fig. 2(a) and $K_{22} = 10$ in Fig. 2(b)] while their concentration is increased from $\varphi_2 = 0.008$ (solid line), to $\varphi_2 = 0.02$ (dashed line), and then to $\varphi_2 = 0.08$ (dotted line). In the case of neutral polymer globules [$K_{22} = 0$, Fig. 2(a)], this process leads to a larger and larger attraction at contact whereas at the same time a no-

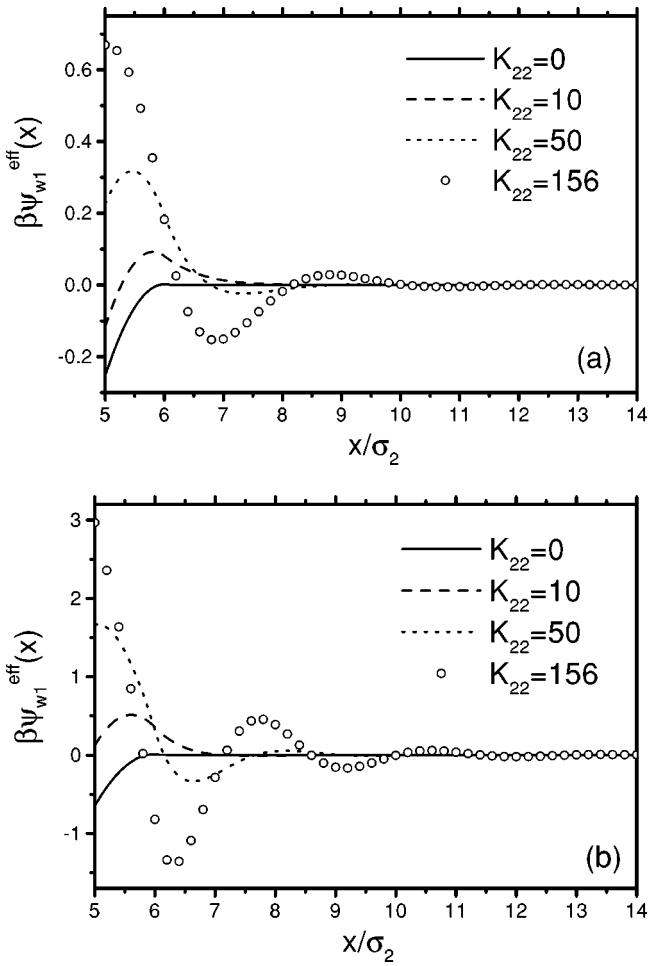

FIG. 1. The figure shows how the wall-particle depletion potential $\beta\psi_{w1}^{\mathrm{eff}}(x)$ changes when the electrostatic repulsion between added macromolecules increases; starting with neutral coils ($K_{22}=0$, solid lines), passing through $K_{22}=10$ (dashed lines) and $K_{22}=50$ (dotted lines), and finally reaching $K_{22}=156$ (circles). The displayed results correspond to the infinite dilute limit of macroparticles ($\varphi_1=0$) in front of a neutral hard wall ($K_{w2}=0$) for two different concentrations of unobserved particles; (a) $\varphi_2=0.008$ and (b) $\varphi_2=0.02$.

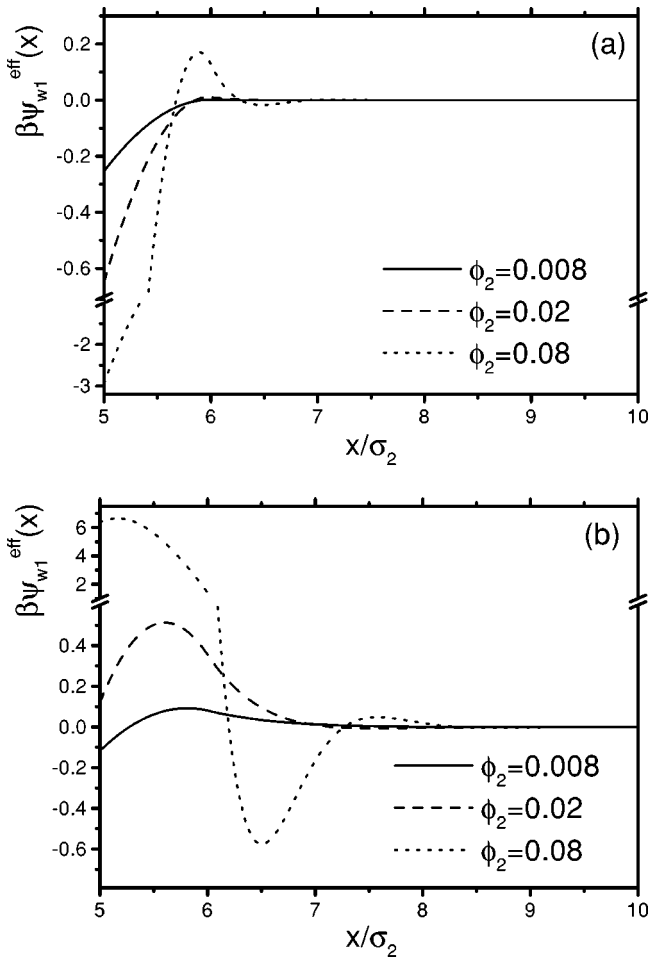

FIG. 2. The figure shows how the wall-particle depletion potential $\beta\psi_{w1}^{\mathrm{eff}}(x)$ changes when the concentration of added macromolecules increases; starting with $\varphi_2=0.008$ (solid lines), passing through $\varphi_2=0.02$ (dashed lines), and finally reaching $\varphi_2=0.08$ (dotted lines). The displayed results correspond to the infinite dilute limit of macroparticles ($\varphi_1=0$) in front of a neutral hard wall ($K_{w2}=0$) for two different values of the electrostatic repulsion between the unobserved particles; (a) $K_{22}=0$ and (b) $K_{22}=10$.

ticeable barrier develops at a distance of roughly σ_2 from contact, i.e., a distance corresponding to the position of the first layer of polymer globules adjacent to the wall, features that have been previously discussed by other authors [6,12]. In the case of charged polymer globules [$K_{22}=10$, Fig. 2(b)] the contact value of $\beta\psi_{w1}^{\mathrm{eff}}(x)$ becomes instead more repulsive when φ_2 is increased, leading to a large barrier in the vicinity of the wall for the maximum value of φ_2 illustrated in Fig. 2(b).

The effects of a finite concentration of macroparticles are illustrated in Figs. 3–6, which show results of the effective wall-particle potentials that correspond to $K_{w2}=0$ (hard wall) and $\varphi_2=0.02$. In particular, Figs. 3, 4, and 5 show the comparison of the results for $\varphi_1=0$ (solid line) with the results corresponding to $\varphi_1=0.2$ (dashed line) for the following values: $K_{22}=0$ (Fig. 3), $K_{22}=10$ (Fig. 4), and $K_{22}=50$ (Fig. 5). In these three figures we can distinguish two separate regions. In the region closest to the wall ($x\lesssim\sigma_1$), the most noticeable change on the shape of $\beta\psi_{w1}^{\mathrm{eff}}(x)$ due to the increment of the macroparticle concentration is again an amplification of the oscillations contained within this region. In the case of neutral unobserved particles (Fig. 3), the attraction at contact becomes deeper and the first peak becomes higher when the concentration of macroparticles is increased. For the cases of charged polymer globules (Figs. 4 and 5), the potential barrier adjacent to the wall becomes more repulsive whereas the first valley becomes more attractive when φ_1 is incremented. Besides, in the second region ($x\gtrsim\sigma_1$) the effective wall-macroparticle potentials in these three figures exhibit an oscillatory, although relatively small, structure in the case of $\varphi_1=0.2$ that is absent in the case of $\varphi_1=0$. The structure of $\beta\psi_{w1}^{\mathrm{eff}}(x)$ in this second region turns out to be roughly similar for the three different values of K_{22}, although once again the amplitude of its oscillations is incremented, while the positions of the corresponding

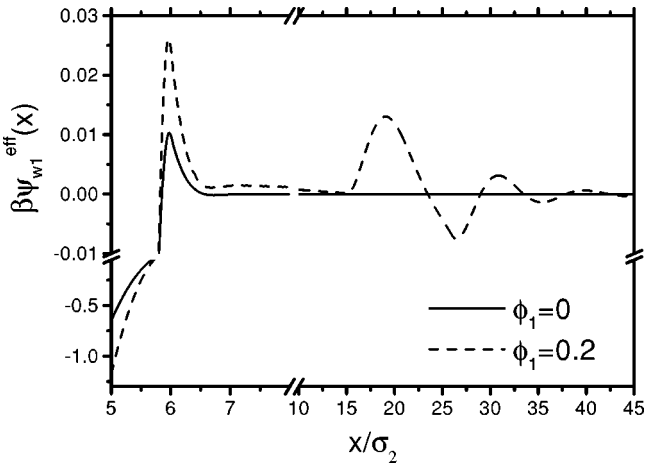

FIG. 3. The figure shows how the wall-particle depletion potential $\beta\psi_{w1}^{\mathrm{eff}}(x)$ changes when the concentration of macroparticles increases; going from $\varphi_1=0$ (solid line) to $\varphi_1=0.2$ (dashed line) in front of a neutral hard wall ($K_{w2}=0$). The displayed results correspond to a concentration $\varphi_2=0.02$ of neutral macromolecules ($K_{22}=0$).

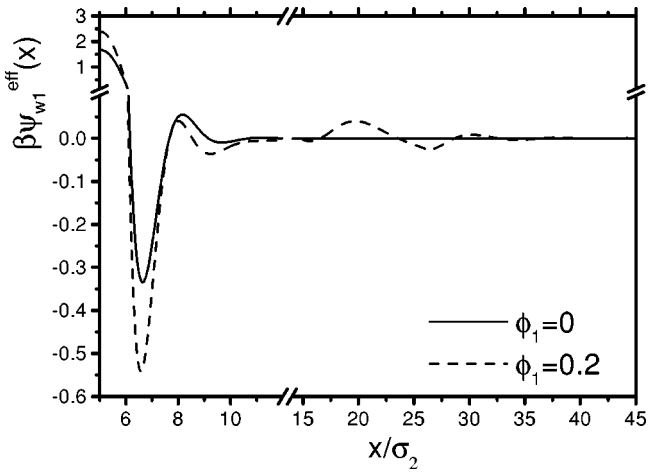

FIG. 5. The figure shows how the wall-particle depletion potential $\beta\psi_{w1}^{\mathrm{eff}}(x)$ changes when the concentration of macroparticles increases; going from $\varphi_1=0$ (solid line) to $\varphi_1=0.2$ (dashed line) on front of a neutral hard wall ($K_{w2}=0$). The displayed results correspond to a concentration $\varphi_2=0.02$ of charged macromolecules ($K_{22}=50$).

maxima and minima remain almost invariant, when this parameter is increased. This feature can be better appreciated in Fig. 6, which shows the comparison of the graphics of the effective wall-macroparticle potentials corresponding to $\varphi_1=0.2$ for $K_{22}=0$ (solid line), $K_{22}=10$ (dashed line), and $K_{22}=50$ (dotted line). An important feature shown in Fig. 6 is the length scale of the oscillations observed in it, which is roughly of the order of σ_1, in contrast with the length scale of the oscillations in the region $x\lesssim\sigma_1$, which is roughly of the order of σ_2. This feature seems to indicate that the long-ranged structure of $\beta\psi_{w1}^{\mathrm{eff}}(x)$ is induced by the ''holes'' in the distribution of unobserved particles created by the presence of the macroparticles. Although the amplitudes of the oscillations observed in Fig. 6 are rather small, it is to be expected that this long-ranged structure will become more relevant for larger values of φ_2.

Finally, Fig. 7 illustrates the process of varying the surface charge density of the wall while keeping fixed all the other parameters. The results presented in this figure correspond to $\varphi_1=0$, $\varphi_2=0.02$, $K_{22}=50$, and to the sequence $K_{w2}=2$ (solid line), $K_{w2}=0$ (dashed line), and $K_{w2}=-2$ (dotted line). As the wall becomes more attractive with regard to the unobserved particles, the effective wall-macroparticle potential becomes ever more repulsive at contact, and even for the relatively narrow range of values of K_{w2} represented in this figure the change on the contact

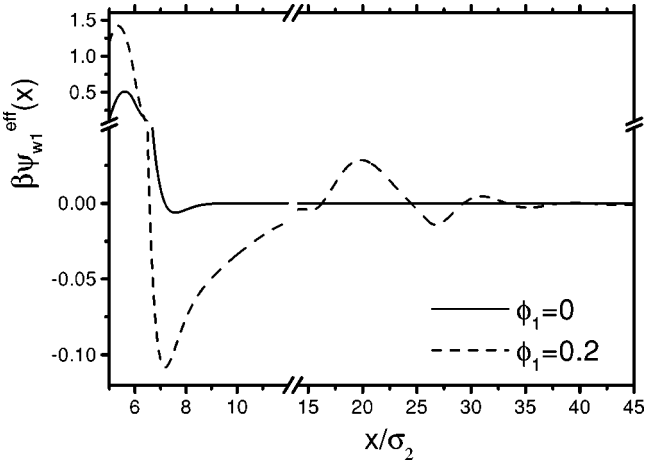

FIG. 4. The figure shows how the wall-particle depletion potential $\beta\psi_{w1}^{\mathrm{eff}}(x)$ changes when the concentration of macroparticles increases; going from $\varphi_1=0$ (solid line) to $\varphi_1=0.2$ (dashed line) in front of a neutral hard wall ($K_{w2}=0$). The displayed results correspond to a concentration $\varphi_2=0.02$ of charged macromolecules ($K_{22}=10$).

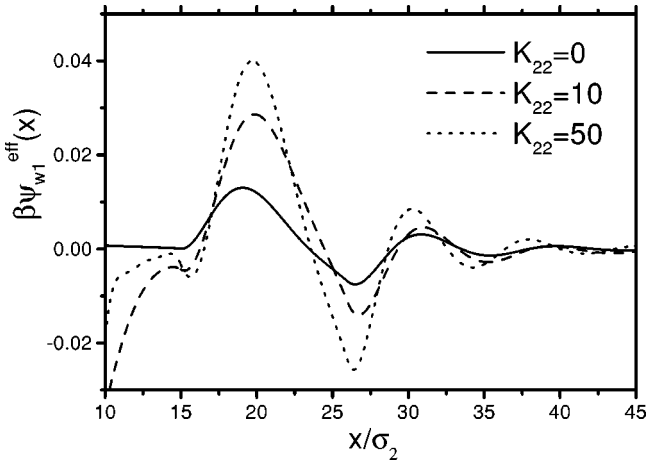

FIG. 6. The figure shows how the wall-particle depletion potential $\beta\psi_{w1}^{\mathrm{eff}}(x)$ in the far region ($x\gtrsim\sigma_1$) changes when the electrostatic repulsion between added macromolecules increases; starting with neutral coils ($K_{22}=0$, solid line), passing through $K_{22}=10$ (dashed line), and finally reaching $K_{22}=50$ (dotted line). The displayed results correspond to the concentration $\varphi_1=0.2$ of macroparticles in front of a neutral hard wall ($K_{w2}=0$), and to a concentration $\varphi_2=0.02$ of unobserved particles.

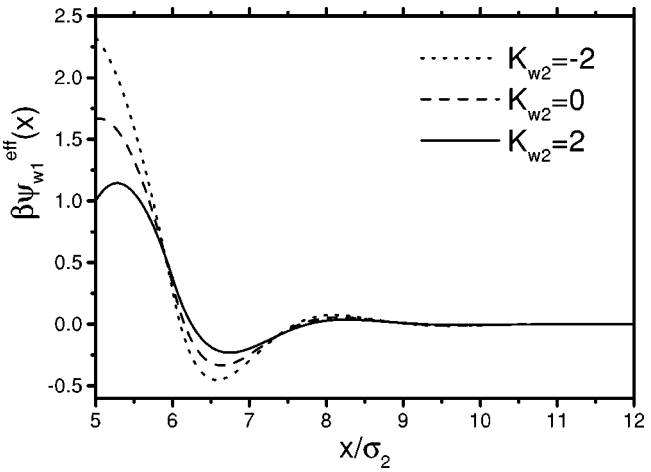

FIG. 7. The figure shows how the wall-particle depletion potential $\beta\psi_{w1}^{\mathrm{eff}}(x)$ changes when the surface charge density of the wall varies; starting with an attractive wall ($K_{w2}=-2$, dotted line), passing through a neutral wall ($K_{w2}=0$, dashed line), and finally reaching a repulsive wall ($K_{w2}=2$, solid line). The displayed results correspond to the infinite dilute limit of macroparticles ($\varphi_1=0$) and to the concentration $\varphi_2=0.02$ of charged macromolecules ($K_{22}=50$).

value of this effective potential turns out to be quite important. This effect is also explained by the larger or smaller number of charged polymer globules located on the surface of the wall when it becomes more attractive or more repulsive, and by the way that these globules in turn push the macroparticles away from the wall. The effective interaction of the wall on the macroparticles is then influenced by the surface charge density of the former even though the macroparticles themselves are neutral.

V. CONCLUSIONS

Recently, it has been shown how depletion potentials arise from contracting the full integral equation theory of a p-component mixture to an effective description on a level which includes explicitly less than p components [12]. In this paper, we extended those results to the case of inhomogeneous systems. In the simplest case of a binary mixture ($p=2$) on the front of a wall one obtains as effective description an inhomogeneous one-component system of particles interacting between them, and with the wall through potentials depending parametrically on the contracted component. The approach developed in this paper is of the same spirit as the one used by Mao, Cates, and Lekkerkerker [32]. Instead of integrating over the degrees of freedom of the small particles in the partition function we follow Ref. [12] and rewrite the Ornstein-Zernike equation for the density profiles (15) in the form of Eq. (18). The effects of the contracted component are then taken care of in the direct correlation functions $c_{11}^{\mathrm{eff}}(r)$ and $c_{w1}^{\mathrm{eff}}(\mathbf{r})$ of the contracted system. The wall-particle depletion potential is obtained from $c_{w1}^{\mathrm{eff}}(\mathbf{r})$ by employing a closure relation; for reasons of simplicity we have used the mean spherical approximation (MSA), but any other more sophisticated closure relation could have been used as well.

The effective direct correlation function $c_{w1}^{\mathrm{eff}}(\mathbf{r})$ is given in terms of the direct correlation functions of the contracted components. Introducing simple approximations for the latter, it has been shown that the Asakura-Oosawa results follow immediately. But our main interest has been to show how these results change when the assumptions of the Asakura-Oosawa theory no longer apply. From the numerical solution of the full set of OZ equations it is possible to calculate the wall-particle depletion potentials for arbitrary concentrations of all components of the mixture. Furthermore, energetic contributions to the depletion forces can also be included in order to describe more realistic systems than that composed by only hard spheres.

Finally, our approach assumes through Eqs. (8) and (20) that depletion forces are pairwise additive. Direct computer simulations by Dijkstra, van Roij, and Evans [33] have recently shown the correctness of this assumption for hard sphere mixtures, even in regimes where one might expect the approximation of pairwise additivity to fail. Although it was still not proven for inhomogeneous mixtures of charged and uncharged particles, we also neglect effective triplet interactions in that case.

ACKNOWLEDGMENT

The authors thank CONACyT-Mexico for financial support (Grant No. 26270-E).

[1] S. Asakura and F. Oosawa, J. Chem. Phys. **22**, 1255 (1954).
[2] A. Vrij, Pure Appl. Chem. **48**, 471 (1976).
[3] U. Steiner, A. Meller, and J. Stavans, Phys. Rev. Lett. **74**, 4750 (1995).
[4] T. Biben and J.P. Hansen, Phys. Rev. Lett. **66**, 2215 (1991).
[5] T. Biben, P. Bladon, and D. Frenkel, J. Phys.: Condens. Matter **8**, 10 799 (1996).
[6] Y. Mao, M.E. Cates, and H.N.W. Lekkerkerker, Physica A **222**, 10 (1995).
[7] B. Götzelmann, R. Evans, and S. Dietrich, Phys. Rev. E **57**, 6785 (1998).
[8] Y. Rosenfeld, Phys. Rev. Lett. **72**, 3831 (1994).
[9] H.H. von Grünberg and R. Klein, J. Chem. Phys. **110**, 5421 (1999).
[10] C. Bechinger (private communication).
[11] R. Garibay-Alonso, J.M. Méndez-Alcaraz, and R. Klein, Physica A **235**, 159 (1997).
[12] J.M. Méndez-Alcaraz and R. Klein, Phys. Rev. E **61**, 4095 (2000).
[13] M. Medina-Noyola and D.A. McQuarrie, J. Chem. Phys. **73**, 6279 (1980).
[14] P. González-Mozuelos and M.D. Carbajal-Tinoco, J. Chem. Phys. **109**, 11 074 (1998).
[15] P. González-Mozuelos, M. Medina-Noyola, B. D'Aguanno,

J.M. Méndez-Alcaraz, and R. Klein, J. Chem. Phys. **95**, 2006 (1991).
[16] P. González-Mozuelos, J. Alejandre, and M. Medina-Noyola, J. Chem. Phys. **95**, 8337 (1991).
[17] P. González-Mozuelos, J. Alejandre, and M. Medina-Noyola, J. Chem. Phys. **97**, 8712 (1992).
[18] P. González-Mozuelos, J. Chem. Phys. **98**, 5747 (1993).
[19] P. González-Mozuelos and J. Alejandre, J. Chem. Phys. **105**, 5949 (1996).
[20] G. Rodríguez and L. Vicente, Mol. Phys. **87**, 213 (1996).
[21] M. Chávez-Páez, H. Acuña-Campa, L. Yeomans-Reyna, M. Valdez-Covarrubias, and M. Medina-Noyola, Phys. Rev. E **55**, 4406 (1997).
[22] M. Chávez-Páez, E. Urrutia-Bañuelos, and M. Medina-Noyola, Phys. Rev. E **58**, 681 (1998).
[23] J.P. Hsu, M.T. Tseng, and S. Tseng, Chem. Phys. **242**, 69 (1999).
[24] M.L. Pollard and C.J. Radke, J. Chem. Phys. **101**, 6979 (1994).
[25] N. Choudhury and S.K. Ghosh, J. Chem. Phys. **104**, 9563 (1996).
[26] N. Choudhury and S.K. Ghosh, J. Chem. Phys. **108**, 7493 (1998).
[27] Y.-W. Kim, S.-C. Kim, and S.-H. Suh, J. Chem. Phys. **110**, 1230 (1999).
[28] J.P. Hansen and I.R. McDonald, *Theory of Simple Liquids* (Academic, London, 1986).
[29] K. Hiroike, J. Phys. Soc. Jpn. **27**, 1415 (1969).
[30] D. Rudhart, C. Bechinger, and P. Leiderer, Phys. Rev. Lett. **81**, 1330 (1998).
[31] K.C. Ng, J. Chem. Phys. **61**, 2680 (1974).
[32] Y. Mao, M.E. Cates, and H.N.W. Lekkerkerker, J. Chem. Phys. **106**, 3721 (1997).
[33] M. Dijkstra, R. van Roij, and R. Evans, Phys. Rev. Lett. **82**, 117 (1999).